

1 Modified Atomic Orbital Theory Applied to the Study of $(3d^9 4s^3 D_{3,2,1})np$ 2 and the $(3d^9 4s^1 D_2)np$ Rydberg series of Cu-like Zn^+ .

3

4 Abstract

5 Precise values of high-lying resonance energies have been determined for the Rydberg series
6 $(3d^9 4s^3 D_{3,2,1})np$ and $(3d^9 4s^1 D_2)np$ (n ranging from 5 to 45), originating from the ground state
7 $(3d^{10} 4s^1 S_{1/2})$ of the Cu-like Zn^+ ion. These calculations were carried out within the framework
8 of the Modified Atomic Orbital Theory (MAOT) method. The results show excellent
9 agreement with high-resolution measurements performed at ALS, as well as with calculations
10 obtained using the DARC codes (*Dirac Atomic R-matrix Codes*) (Hinojosa et al., *MNRAS*,
11 470, 4048 (2017)). The analysis is based both on standard quantum defect theory and on the
12 MAOT procedure, which relies on the calculation of the effective charge. The study highlights
13 the relevance of the MAOT method in complementing experimental data, particularly for the
14 accurate identification of narrow resonance energies affected by overlapping spectral
15 peaks. Finally, new accurate resonance energies for high-lying levels ($n = 16 - 45$) are
16 proposed as benchmark data to aid in the interpretation of spectra from trans-iron elements in
17 astrophysical environments.

18

19 Keywords

20 Photoionization, Resonance Energies, Quantum Defect, Modified Atomic Orbital Theory,
21 Rydberg Series, Synchrotron Radiation

22

23 1. Introduction

24 Resonant photoionization (PI) is a fundamental process in which a photon excites an atom or
25 ion to an unstable intermediate electronic state (autoionizing), which subsequently decays by
26 emitting a free electron. This mechanism leads to a strong enhancement of photoionization
27 cross sections and gives rise to characteristic resonant structures in the spectra.

28 In astrophysical plasmas, such as stellar atmospheres and interstellar media enriched in heavy
29 metals, zinc PI plays a key role in the ionization balance and in determining chemical
30 abundances. Zinc, particularly in the form of Zn II and Zn III ions, is used as an astrophysical
31 tracer since it is only weakly affected by depletion onto interstellar dust. Thus, the study of
32 resonant photoionization of zinc provides constraints on the chemical composition and
33 evolution of stars and galaxies based on UV observations (e.g., with *HST* and *FUSE*) (Ferland
34 et al., 1998; Kallman & Palmeri, 2007).

35 In laboratory plasmas, resonant photoionization of zinc is investigated using synchrotron light
36 sources (*ALS, SOLEIL, PETRA III*), allowing high-resolution measurements of PI cross
37 sections for different ions (Zn II, Zn III, Zn IV). These experimental measurements provide
38 essential benchmark data to test and validate advanced theoretical models (*R-matrix*, Dirac
39 Atomic R-matrix Codes – DARC, and semi-empirical methods such as SCUNC) (Peart et al.,
40 1987; Hinojosa et al., 2017; Sakho, 2017, 2018). These studies are also applied to plasma
41 diagnostics and the production of highly charged ions in laboratory physics.

42 Although high-resolution ALS measurements have been conducted and compared with
43 advanced DARC calculations, many spectral peaks of Zn⁺ ions remain overlapping, and the
44 corresponding resonances have not been clearly identified. The Modified Atomic Orbital
45 Theory(MAOT) method (Diallo et al. 2018,2025; Sakho, 2011) has proven to be a highly
46 suitable semi-empirical method for accurately reproducing experimental photoionization data.
47 The aim of the present study is to clarify the overlapping ALS lines by using the MAOT
48 method to calculate resonance energies of the (3d⁹ 4s D₃)*np*, (3d⁹ 4s ³D₂)*np*, (3d⁹ 4s ³D₁)*np*,
49 and (3d⁹ 4s ¹D₂)*np* Rydberg series of Zn⁺ ions. Moreover, high-lying Rydberg series provide
50 valuable data for the NIST database, where many resonances are tabulated up to n= 60 for
51 atomic systems such as Mg. This work also aims to extend the ALS measurements (Hinojoh
52 et al., 2017) and associated DARC calculations to higher principal quantum numbers, *n* =
53 16 – 45.

54 The analysis of the present results is carried out within the framework of standard quantum-
55 defect theory and the MAOT procedure, through calculation of the effective charge. The
56 organization of this paper is as follows. Section 2 provides a brief overview of the MAOT
57 formalism, while Section 3 presents the results. The study is concluded in Section 4.

58

59 **2. Theory**

60 **2.1. Brief description of the MAOT formalism**

61 In the framework of the modified atomic orbital theory (MAOT), the total energy of a (*νl*)-
62 given orbital is expressed in the form in Rydberg units (Diallo et al., 2018,2025).

$$63 \quad E(\nu l) = -\frac{[Z - \sigma(l)]^2}{\nu(l)^2} \quad (1)$$

64 The details of this Equation1 are given in our previous papers (Diallo et al., 2025). In the
65 photoionization study, energy resonances *E_n* are generally measured relatively to the *E_∞*

66 converging limit of a given ($^{2S+1}L_J$) nl - Rydberg series. General expression of the resonance
 67 energy E_n is given by (inRydberg units):

$$68 \quad E_n = E_\infty - \frac{1}{n^2} \left\{ Z - \sigma_1(^{2S+1}L_J) - \sigma_2(^{2S+1}L_J) \times \frac{1}{n} - \sigma_2^\alpha(^{2S+1}L_J) \times (n-m) \times (n-q) \sum_k \frac{1}{f_k(n, m, q, s)} \right\}^2 \quad (2)$$

69 In this equation (2), m and q ($m < q$) denote the principal quantum numbers of the ($^{2S+1}L_J$) nl -
 70 Rydberg series of the considered atomic system used in the empirical determination of the
 71 $\sigma_i(^{2S+1}L_J)$ - screening constants, s represents the spin of the nl -electron ($s = 1/2$), E_∞ is the
 72 energy value of the series limit generally determined from NIST atomic database, Z represents
 73 the nuclear charge of the considered element and $\sum_k \frac{1}{f_k(n, m, q, s)}$ is a corrective term

74 introduced to stabilize expression (2). The only problem that one may face by using the
 75 MAOT

76 formalism is linked to the determination of the $\sum_k f_k(n, m, q, s)$ -terme. The correct expression
 77 of this term is determined iteratively by imposing the general Eq. (2) to provide accurate data
 78 with nearly constant or slightly varying quantum defect values along all considered series as
 79 the principal quantum number n increases. The value of α is fixed to 1 and or 2 during the
 80 iteration.

81

82 2.2. Quantum Defect of MOAT

83 In general, resonance energies are analyzed from the standard quantum-defect expansion
 84 formula

$$85 \quad E_n = E_\infty - \frac{RZ_{core}^2}{(n - \delta_n)^2} \quad (3)$$

86 In this equation, $R=13,60569\text{eV}$ is the Rydberg constant, E_∞ denotes the converging limit,
 87 Z_{core} represents the electric charge of the core ion, and δ means the quantum defect.

88 From (3), the quantum defect δ_n is calculated as follows:

$$89 \quad \delta_n = n - Z_{core} \sqrt{\frac{R}{(E_\infty - E_n)}}$$

90 (4)

91 In addition, introducing the effective nuclear charge Z^* , Eq. (2) can be rewritten in the form
 92 of Eq. (3) as follows

93
$$E_n = E_\infty - \frac{Z^{*2}}{n^2} R \quad (5)$$

94 With Z^* given by

95
$$Z^* = \left\{ Z - \sigma_1(2^{S+1}L_J) - \sigma_2(2^{S+1}L_J) \times \frac{1}{n} - \sigma_2^\alpha(2^{S+1}L_J) \times (n-m) \times (n-q) \sum_k \frac{1}{f_k(n,m,q,s)} \right\}$$

96 (6)

97 When n tend toward infinity, Eq. (6) tends to the limit

98
$$Z_{Lim}^* = Z_{core} = \{Z - \sigma_1(2^{S+1}L_J)\} \Rightarrow \sigma_1(2^{S+1}L_J) = Z - Z_{core}$$

99 (7)

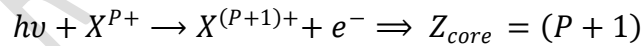
100 where Z_{core} is the effective core charge.

101 In the present work, for all the Rydberg series investigated for both Zn II, the resonance
102 energies are given by the formula

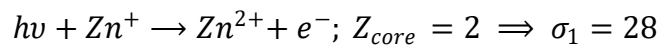
$$E_n = E_\infty - \frac{1}{n^2} \left\{ Z - \sigma_1 - \sigma_2 \times \frac{1}{n} - \sigma_2^2 \times \frac{(n-m) \times (m-4s-s^2)}{n^2 \times (n+5m+s)} \right\}^2 Ryb \quad (8)$$

103 3. Results and Discussion

104 The σ_2 screening constants in Equations (6) and (8) were determined empirically, based on
105 the experimental data reported by Hinojosa et al.(2017). The corresponding values are
106 presented in the table caption. In contrast, the σ_2 screening constant was obtained theoretically
107 from the simple relation $\sigma_1 = Z - Z_{core}$, where the effective core charge (Z_{core}) is directly
108 deduced from the single photoionization process of a given X^{P+} plasma ion.



109 So, for Cu-like Zn II ion, we find.



110 The resonance energies of the I ($3d^94s \ ^3D_3$) np , II ($3d^94s \ ^3D_2$) np , III ($3d^94s \ ^3D_1$) np , IV ($3d^94s$
111 $\ ^1D_2$) np , and V ($3d^94s \ ^3D_3$) np Rydberg series, originating from the ($3d^{10}4s$) $\ ^1S_{1/2}$ ground state
112 of Zn^+ ions, are reported in **Tables 1–5**. The present MAOT calculations are compared with
113 results obtained using the SCUNC method (Badiane et al., 2019) as well as with ALS
114 experimental data (Hinojoha et al., 2017). In the ALS studies, resonance energies were
115 determined only up to $n = 15$ (see Table 4). Generally, because of configuration interaction
116 and electron–electron correlation effects, cross-section peaks tend to overlap, making the

117 identification of spectral lines increasingly difficult as n increases. Nevertheless, the MAOT
118 approach proves sufficiently stable to tabulate very high-lying resonances up to $n = 45$, with
119 the quantum defect remaining nearly constant across all the series investigated. Furthermore,
120 for several resonances, uncertain experimental entries indicated in parentheses are clarified.
121 **Table 1** presents the quantum defects and resonance energies of the $(3d^94s\ ^3D_3)np$ Rydberg
122 series, originating from the $3d^{10}4s\ ^1S_{1/2}$ ground state of Zn^+ and converging to the $(3d^94s\ ^3D_3)$
123 series limit of Zn^{2+} . Four uncertain ALS values are reported for the 7p, 9p, 11p, and 12p levels
124 at [26.093 eV], [26.773 eV], [27.087 eV], and [27.184 eV], respectively. These are compared
125 with the present MAOT predictions of 26.097 eV, 26.778 eV, 27.092 eV, and 27.189 eV, and
126 with the SCUNC results of Badiane et al. (2019), which give 26.102 eV, 26.782 eV, 27.095
127 eV, and 27.192 eV. The maximum discrepancy between ALS data and the new MAOT
128 calculations is 0.005 eV, while it rises to 0.009 eV in the values of Badiane et al. (2019). For
129 $n = 6$ and 8 , the MAOT energies (25.409 eV and 26.510 eV) show excellent agreement with
130 ALS measurements (25.408 eV and 26.512 eV; Hinojoha et al., 2017). Across all resonances,
131 the MAOT quantum defect remains nearly constant, ranging from 1.1 to 1.2, consistent with
132 the ALS average value of 1.11 ± 0.2 (Hinojoha et al., 2017). **Tables 2 and 3** lists resonance
133 energies and quantum defects of the Rydberg series $(3d^94s\ ^3D_2)np$ and $(3d^94s\ ^3D_1)np$,
134 originating from the ground state $(3d^{10}4s)\ ^1S_{1/2}$ of Zn^+ ions and converging respectively to the
135 $(3d^94s\ ^3D_2)$ and $(3d^94s\ ^3D_1)$ series limits of Zn^{2+} . The results obtained with the MAOT method
136 are compared with ALS experimental measurements (Hinojoha et al., 2017) as well as with
137 the SCUNC predictions (Badiane et al., 2019). For the $(3d^94s\ ^3D_2)np$ and $(3d^94s\ ^3D_1)np$ series,
138 uncertain ALS values were identified at the 10p and 9p states, with corresponding energies of
139 [27.104 eV] and [27.116 eV]. The MAOT predictions for these states are 27.108 eV and
140 27.121 eV, yielding deviations of only 0.004 eV and 0.005 eV, respectively, from the ALS
141 data. For the remaining resonances between $n = 5$ and $n = 10$, the agreement between theory
142 and experiment is excellent, with energy differences never exceeding 0.008 eV. Moreover, the
143 quantum defect predicted by MAOT remains nearly constant, ranging between 1.1 and 1.2.
144 Finally, for the two $(3d^94s\ ^3D)np$ Rydberg series originating from the ground state $(3d^{10}4s\ ^1S_{1/2})$
145 of Zn^+ , the MAOT results are extended up to $n = 45$, confirming an almost invariant
146 quantum defect throughout the series. In the **Table 4** we have the resonance energies and
147 quantum defect of the $(3d^94s\ ^1D_2)np$ Rydberg series, originating from the $(3d^{10}4s\ ^1S_{1/2})$ ground
148 state of the Zn^+ ion and converging to the $(3d4s\ ^1D_2)$ series limit of Zn^{2+} . The results obtained
149 using the MAOT method are compared with ALS experimental data (Hinojoha et al., 2017) as
150 well as with the theoretical predictions of the SCUNC model (Badiane et al., 2019). Three

151 characteristic resonances $(3d^9 4s^1 D_2)6p$, $(3d^9 4s^1 D_2)7p$, and $(3d^9 4s^1 D_2)8p$ are identified as
152 overlapping states. Their resonance energies, 26.080 eV, 26.769 eV, and 27.183 eV,
153 respectively, are in close agreement with both the MAOT predictions (26.081 eV, 26.770 eV,
154 and 27.184 eV) and those from the SCUNC model. For the $(3d^9 4s^1 D_2)8p$ state, the MAOT
155 value shows particularly good agreement with experiment, with a deviation of only 0.001 eV,
156 compared to 0.006 eV for the SCUNC prediction, confirming the reliability of this
157 result. Except for the $(3d^9 4s^1 D_2)6p$ state, which shows a shift of 0.011 eV, the maximum
158 discrepancy between the new calculations and the experimental data remains below 0.07 eV.
159 For levels $n = 9$ to 15, the agreement between MAOT values and ALS measurements is
160 excellent, with differences never exceeding 0.006 eV. Finally, the quantum defect of this
161 Rydberg series remains nearly constant, between 1.1 and 1.2. **Table 5** shows the resonance
162 energies and quantum defects of the $(3d^9 4s^3 D_3)np$ Rydberg series, originating from the
163 $(3d^{10} 4s^1 S_{1/2})$ ground state of the Zn^+ ion and converging to the $(3d^9 4s^3 D_3)$ series limit of Zn^{2+} .
164 The results obtained using the MAOT method are compared with the experimental ALS
165 measurements (Hinojosa et al., 2017). For this series, two overlapping resonances were
166 identified, corresponding to the 8p and 9p states, located at 26.340 eV and 26.714 eV,
167 respectively. The MAOT predictions for these levels are 26.404 eV and 26.711 eV, yielding a
168 maximum energy difference of 0.064 eV. It is worth noting that the SCUNC method (Badiane
169 et al., 2019) encountered difficulties in providing reliable data for this series, highlighting the
170 relevance of the MAOT predictions as a reference for future high-resolution measurements.
171 Finally, for all resonances considered, the quantum defect remains nearly constant, within the
172 range 1.4-1.5. **Tables 6 and 7** compare resonance energies of the $(3d^9 4s^3 D_3)np$ and $(3d^9 4s^3 D_2)np$
173 $^3 D_2)np$ series, as well as the $(3d^9 4s^3 D_1)np$ and $(3d^9 4s^1 D_2)np$ series, all originating from the
174 $3d^{10} 4s^1 S_{1/2}$ ground state of Zn^+ and converging respectively to the $(3d^9 4s^3 D_3)$ and $(3d^9 4s^3 D_2)$
175 limits of Zn^{2+} . The present MAOT results are compared with ALS measurements, the Dirac-
176 Coulomb R-matrix (DARC) calculations of Hinojosa et al. (2017), and the pioneering
177 merged-beams experiments of Peart et al. (1987) conducted at the Daresbury synchrotron
178 facility. The comparison indicates that MAOT predictions agree more closely with ALS data
179 than other theoretical approaches. The maximum relative deviation is only 0.04% for the
180 $(3d^9 4s^3 D_3)7p$ state, mainly due to experimental uncertainties in the ALS value [26.093 eV].
181 In contrast, the DARC method shows a deviation of 0.07% for the same state, while the DAR
182 approach exhibits a larger deviation of 0.24% at the $(3d^9 4s^3 D_2)7p$ level.

183 **Tableau 1:** Resonance energies (E) and quantum defect (δ) of the $(3d^9 4s^3 D_3)np$ Rydberg
 184 series I originate from the $(3d^{10} 4s) ^1S_{1/2}$ ground state of the Zn^+ ions converging to the $(3d^9 4s$
 185 $^3D_3)$ series limit of Zn^{2+} . The present MAOT results are compared with the SCUNC results
 186 (Badiane et al., 2017) and the ALS experimental data (Hinojoha et al., 2017). The ALS
 187 energies are calibrated to $\pm 0,017$ eV. $\sigma_1(2D5/2) = -0.770 \pm 0.048$; $\sigma_2(2D5/2) = 28.00$.

		$I(3d^9 4s^3 D_3)np$				
n	δ	MAOT	SCUNC	ALS	MAOT	SCUNC
		E	E	E	$ \Delta E $	$ \Delta E $
5	1,1	24,141	24,141	24,141	0.000	0.000
6	1,1	25,409	25,415	25,408	0.001	0.007
7	1,1	26,097	26,102	[26,093]	[0.004]	[0.009]
8	1,1	26,510	26,515	26,512	0.002	0.003
9	1,1	26,778	26,782	[26,773]	[0.005]	[0.009]
10	1,1	26,961	26,965	26,966	0.005	0.001
11	1,1	27,092	27,096	[27,087]	0.005	[0.008]
12	1,1	27,189	27,192	[27,184]	0.005	[0.008]
13	1,1	27,262	27,265	(27,253)	(0.009)	(0.012)
14	1,1	27,320	27,321			
15	1,1	27,365	27,367			
16	1,1	27,401	27,403			
17	1,1	27,431	27,433			
18	1,1	27,456	27,457			
19	1,1	27,477	27,478			
20	1,1	27,494	27,495			
21	1,1	27,509	27,510			
22	1,1	27,522	27,523			
23	1,1	27,533	27,534			
24	1,1	27,543	27,543			
25	1,1	27,551	27,552			
26	1,2	27,559	27,559			
27	1,2	27,566	27,566			
28	1,2	27,571	27,572			
29	1,2	27,577	27,577			
30	1,2	27,582	27,582			
31	1,2	27,586	27,586			
32	1,2	27,590	27,590			
33	1,2	27,593	27,594			
34	1,2	27,596	27,597			
35	1,2	27,599	27,600			
36	1,2	27,602	27,602			
37	1,2	27,605	27,605			
38	1,2	27,607	27,607			
39	1,2	27,609	27,609			
40	1,2	27,611	27,611			
41	1,2	27,613	-			
42	1,2	27,614	-			
43	1,2	27,616	-			
44	1,2	27,617	-			
45	1,2	27,619	-			

188 **Tableau 2:** Resonance energies (E) and quantum defect (δ) of the $(3d^9 4s^3 D_2)np$ Rydberg
 189 series II originate from the $(3d^{10} 4s) ^1S_{1/2}$ ground state of the Zn^+ ions converging to the $(3d^9 4s$
 190 $^3D_2)$ series limit of Zn^{2+} . The present MAOT results are compared with the SCUNC results
 191 (Badiane et al., 2017) and the ALS experimental data (Hinojoha et al., 2017). The ALS
 192 energies are calibrated to $\pm 0,017$ eV.

		II($3d^9 4s^3 D_2$) np				
n	δ	MAOT	SCUNC	ALS	MAOT	SCUNC
		E	E	E	$ \Delta E $	$ \Delta E $
5	1,1	24,294	24,294	24,294	0.000	0.000
6	1,1	25,559	25,564	25,569	0.010	0.005
7	1,1	26,245	26,250	26,243	0.002	0.007
8	1,1	26,658	26,662	26,656	0.002	0.006
9	1,1	26,925	26,929	26,926	0.001	0.003
10	1,1	27,108	27,112	[27,104]	[0.004]	[0.008]
11	1,1	27,239	27,242			
12	1,1	27,335	27,338			
13	1,1	27,409	27,411			
14	1,1	27,466	27,468			
15	1,1	27,511	27,513			
16	1,1	27,547	27,549			
17	1,1	27,577	27,579			
18	1,1	27,602	27,603			
19	1,1	27,623	27,623			
20	1,1	27,640	27,641			
21	1,1	27,655	27,656			
22	1,1	27,668	27,669			
23	1,1	27,679	27,680			
24	1,1	27,689	27,690			
25	1,1	27,697	27,698			
26	1,2	27,705	27,705			
27	1,2	27,712	27,712			
28	1,2	27,717	27,718			
29	1,2	27,723	27,723			
30	1,2	27,728	27,728			
31	1,2	27,732	27,732			
32	1,2	27,736	27,736			
33	1,2	27,739	27,740			
34	1,2	27,743	27,743			
35	1,2	27,745	27,746			
36	1,2	27,748	27,748			
37	1,2	27,751	27,751			
38	1,2	27,753	27,753			
39	1,2	27,755	27,755			
40	1,2	27,757	27,757			
41	1,2	27,759	-			
42	1,2	27,760	-			
43	1,2	27,762	-			
44	1,2	27,763	-			
45	1,2	27,765	-			

193 **Tableau 3:** Resonance energies (E) and quantum defect (δ) of the $(3d^9 4s^3 D_1)np$ Rydberg
 194 series III originate from the $(3d^{10} 4s) ^1S_{1/2}$ ground state of the Zn^+ ions converging to the
 195 $(3d^9 4s^3 D_1)$ series limit of Zn^{2+} . The present MAOT results are compared with the SCUNC
 196 results (Badiane et al., 2017) and the ALS experimental data (Hinojoha et al., 2017). The ALS
 197 energies are calibrated to $\pm 0,017$ eV.

		III($3d^9 4s^3 D_1$) np				
n	δ	MAOT	SCUNC	ALS	MAOT	SCUNC
		E	E	E	$ \Delta E $	$ \Delta E $
5	1,1	24,488	24,488	24,488	0.000	0.000
6	1,1	25,754	25,759	25,752	0.002	0.007
7	1,1	26,440	26,446	26,439	0.001	0.007
8	1,1	26,853	26,858	26,858	0.005	0.000
9	1,1	27,121	27,125	[27,116]	[0.005]	[0.009]
10	1,1	27,304	27,307			
11	1,1	27,435	27,438			
12	1,1	27,531	27,534			
13	1,1	27,605	27,607			
14	1,1	27,662	27,664			
15	1,1	27,707	27,709			
16	1,1	27,743	27,745			
17	1,1	27,773	27,775			
18	1,1	27,798	27,799			
19	1,1	27,819	27,820			
20	1,1	27,836	27,837			
21	1,1	27,851	27,852			
22	1,1	27,864	27,865			
23	1,1	27,875	27,876			
24	1,1	27,885	27,885			
25	1,1	27,893	27,894			
26	1,2	27,901	27,901			
27	1,2	27,908	27,908			
28	1,2	27,913	27,914			
29	1,2	27,919	27,919			
30	1,2	27,924	27,924			
31	1,2	27,928	27,928			
32	1,2	27,932	27,932			
33	1,2	27,935	27,936			
34	1,2	27,939	27,939			
35	1,2	27,941	27,942			
36	1,2	27,944	27,944			
37	1,2	27,947	27,947			
38	1,2	27,949	27,949			
39	1,2	27,951	27,951			
40	1,2	27,953	27,953			
41	1,2	27,955	-			
42	1,2	27,956	-			
43	1,2	27,958	-			
44	1,2	27,959	-			
45	1,2	27,961	-			

198 **Tableau 4:** Resonance energies (E) and quantum defect (δ) of the $(3d^9 4s^1 D_2)np$ Rydberg
 199 series IV originate from the $(3d^{10} 4s) ^1S_{1/2}$ ground state of the Zn^+ ions converging to the
 200 $(3d^9 4s^1 D_2)$ series limit of Zn^{2+} . The present MAOT results are compared with the SCUNC
 201 results (Badiane et al., 2017) and the ALS experimental data (Hinojoha et al., 2017). The ALS
 202 energies are calibrated to $\pm 0,017$ eV.

		IV($3d^9 4s^1 D_2$)np				
n	δ	MAOT	SCUNC	ALS	MAOT	SCUNC
		E	E	E	$ \Delta E $	$ \Delta E $
5	1,1	24,804	24,804	24,804	0.000	0.000
6	1,1	26,080	26,081	[26,069]	[0.011]	[0.012]
7	1,1	26,769	26,770	[26,773]	[0.004]	[0.003]
8	1,1	27,183	27,178	[27,184]	[0.001]	[0.006]
9	1,1	27,450	27,451	27,450	0.000	0.001
10	1,1	27,633	27,634	27,632	0.001	0.002
11	1,1	27,764	27,765	27,767	0.003	0.002
12	1,1	27,860	27,861	27,863	0.003	0.002
13	1,1	27,933	27,934	27,939	0.006	0.005
14	1,1	27,990	27,991	27,994	0.004	0.003
15	1,1	28,035	28,036	28,041	0.006	0.005
16	1,1	28,072	28,072			
17	1,1	28,102	28,102			
18	1,1	28,126	28,126			
19	1,1	28,147	28,147			
20	1,1	28,164	28,164			
21	1,1	28,179	28,179			
22	1,1	28,192	28,192			
23	1,1	28,203	28,203			
24	1,1	28,213	28,213			
25	1,1	28,221	28,221			
26	1,2	28,229	28,229			
27	1,2	28,236	28,236			
28	1,2	28,242	28,242			
29	1,2	28,247	28,247			
30	1,2	28,252	28,252			
31	1,2	28,256	28,256			
32	1,2	28,260	28,260			
33	1,2	28,263	28,263			
34	1,2	28,267	28,267			
35	1,2	28,269	28,269			
36	1,2	28,272	28,272			
37	1,2	28,275	28,275			
38	1,2	28,277	28,277			
39	1,2	28,279	28,279			
40	1,2	28,281	28,281			
41	1,2	28,283	-			
42	1,2	28,284	-			
43	1,2	28,286	-			
44	1,2	28,287	-			
45	1,2	28,289	-			

203 **Tableau 5:** Resonance energies (E) and quantum defect (δ) of the $(3d^9 4s^3 D_3)np$ Rydberg
 204 series V originate from the $(3d^{10} 4s) ^1S_{1/2}$ ground state of the Zn^+ ions converging to the $(3d^9 4s$
 205 $^3D_3)$ series limit of Zn^{2+} . The present MAOT results are compared with the SCUNC results
 206 (Badiane et al., 2017) and the ALS experimental data (Hinojoha et al., 2017). The ALS
 207 energies are calibrated to $\pm 0,017$ eV.

$V(3d^9 4s^3 D_3)np$				
n	δ	MAOT	ALS	$ \Delta E $
		E	E	
6	1,4	25,071	25,071	0,000
7	1,4	25,917	25,910	0,007
8	1,4	26,404	(26,340)	(0,064)
9	1,4	26,711	(26,714)	(0,003)
10	1,4	26,916		
11	1,4	27,061		
12	1,4	27,166		
13	1,4	27,245		
14	1,4	27,306		
15	1,4	27,354		
16	1,4	27,393		
17	1,4	27,424		
18	1,4	27,450		
19	1,4	27,472		
20	1,4	27,490		
21	1,4	27,505		
22	1,4	27,519		
23	1,4	27,530		
24	1,5	27,540		
25	1,5	27,549		
26	1,5	27,557		
27	1,5	27,564		
28	1,5	27,570		
29	1,5	27,575		
30	1,5	27,580		
31	1,5	27,585		
32	1,5	27,589		
33	1,5	27,592		
34	1,5	27,596		
35	1,5	27,599		
36	1,5	27,601		
37	1,5	27,604		
38	1,5	27,606		
39	1,5	27,608		
40	1,5	27,610		
41	1,5	27,612		
42	1,5	27,614		
43	1,5	27,615		
44	1,5	27,617		
45	1,5	27,618		

209 **Tableau 6:** Comparison of resonance energies of the $(3d^9 4s^3 D_3)np$ and $(3d^9 4s^3 D_2)np$
 210 Rydberg series originating from the $(3d^{10} 4s) ^1S_{1/2}$ ground state of the Zn^+ ions converging to
 211 the $(3d^9 4s^3 D_3)$ and $(3d^9 4s^3 D_2)$ series limits respectively of Zn^{2+} .

n	$(3d^9 4s^3 D_3)np$ Rydberg series				$(3d^9 4s^3 D_2)np$ Rydberg series			
	MAOT E	DARC E	ALS E	DAR E	MAOT E	DARC E	ALS E	DAR E
5	24,141	24,158	24,141	24,172	24,294	24,312	24,294	24,329
6	25,409	25,418	25,408	25,468	25,559	25,577	25,569	25,616
7	26,097	26,102	[26,093]	26,150	26,245	26,251	26,243	26,305
8	26,510		26,512		26,658		26,656	
9	26,778		[26,773]		26,925		26,926	
10	26,961		26,966		27,108		[27,104]	
11	27,092		[27,087]		27,239			
12	27,189		[27,184]		27,335			
13	27,262		(27,253)		27,409			

212 MAOT, Modified Atomic Orbital Theory, present calculations.

213 DARC, Dirac Atomic R-matrix Codes, (Hinojoha et al., 2017).

214 ALS, experimental results, (Hinojoha et al., 2017).

215 DAR, DARESBURY, experimental results (Peart et al., 1987).

216

217

218 **Tableau 7:** Comparison of resonance energies of the $(3d^9 4s^3 D_1)np$ and $(3d^9 4s^1 D_2)np$
 219 Rydberg series originating from the $(3d^{10} 4s) ^1S_{1/2}$ ground state of the Zn^+ ions converging to
 220 the $(3d^9 4s^3 D_1)$ and $(3d^9 4s^1 D_2)$ series limits respectively of Zn^{2+} .

n	$(3d^9 4s^3 D_1)np$ Rydberg series				$(3d^9 4s^1 D_2)np$ Rydberg series			
	MAOT E	DARC E	ALS E	DAR E	MAOT E	DARC E	ALS E	DAR E
5	24,488	24,504	24,488	24,509	24,804	24,824	24,804	24,839
6	25,754	25,762	25,752	25,786	26,080		[26,069]	
7	26,440		26,439		26,769		[26,773]	
8	26,853		26,858		27,183		[27,184]	
9	27,121		[27,116]		27,450		27,450	
10	27,304				27,633		27,632	
11	27,435				27,764		27,767	
12	27,531				27,860		27,863	
13	27,605				27,933		27,939	
14	27,662				27,990		27,994	
15	27,707				28,035		28,041	

221 MAOT, Modified Atomic Orbital Theory, present calculations.

222 DARC, Dirac Atomic R-matrix Codes, (Hinojoha et al., 2017).

223 ALS, experimental results, (Hinojoha et al., 2017).

224 DAR, DARESBURY, experimental results (Peart et al., 1987).

225

226

227 **4. Conclusion**

228 The Modified Atomic Orbital Theory (MAOT) formalism has been applied to the
229 photoionization study of the $(3d^9 4s \ ^3D_{3, 2, 1})np$ and $(3d^9 4s \ ^1D_2)np$ ($n = 5 - 45$) Rydberg
230 series, originating from the $(3d^{10} 4s \ ^1S_{1/2})$ ground state of the Zn^+ ion. Overall, the results
231 obtained show excellent agreement with high-resolution ALS measurements, as well as with
232 Dirac–Coulomb R-matrix calculations [(Hinojosa et al., 2017), *MNRAS*, 000, 1] and
233 theoretical predictions from the SCUNC method (Badiane et al., 2019). This work
234 demonstrates the ability of the MAOT approach to support experiments in resolving very
235 closely spaced resonance energies, particularly in the presence of overlapping peaks. The
236 newly determined resonance energies, obtained with high precision, are proposed as reference
237 data for the interpretation of Zn^+ spectra observed in nebulae. Furthermore, these high-lying
238 Rydberg series provide a valuable contribution to the enrichment of the NIST atomic
239 database.

240 **FUNDING:**

241 This research received no funding.

242 **DATA AVAILABILITY**

243 All data generated or analyzed during this study are included in this published article.

244 **CONFLICT OF INTEREST**

245 The authors of this work declare that they have no conflicts of interest

246 **Références**

- 247 1. Ba, M. D., et al. (2018). *Radiation Physics and Chemistry*, 153, 111–119.
- 248 2. Diallo et al., (2018). *M. Jour. Mod. Phys.* 9, 2594
- 249 3. Diallo et al., (2025). *Nuclear Science*, Vol. 10, No. 1, pp. 1-14,
- 250 4. Ferland, G. J., et al. (1998). *The 1995 release of Cloudy*. PASP, 110, 761.
- 251 5. Goyal, A., et al. (2016). *Radiation Physics and Chemistry*, 125, 50–57.
- 252 6. Hinojosa, G., et al. (2017). *Monthly Notices of the Royal Astronomical Society*, 470(4),
253 4048–4060.
- 254 7. Kallman, T., & Palmeri, P. (2007). *Atomic data for X-ray astrophysics*. Reviews of
255 Modern Physics, 79, 79.
- 256 8. Khatri, I., et al. (2016). *Radiation Physics and Chemistry*, 130, 208–215.
- 257 9. Langanke, K., & Wiescher, M. (2001). *Reports on Progress in Physics*, 64(12), 1657–
258 1701.
- 259 10. Osterbrock, D. E., & Ferland, G. J. (2006). *Astrophysics of Gaseous Nebulae and*
260 *Active Galactic Nuclei*. University Science Books.
- 261 11. Peart, B., Lyon, I. C., & Dolder, K. I. (1987). *Journal of Physics B: Atomic and*
262 *Molecular Physics*. 20, 5403.

- 263 12. Sakho, I., 2017. *J. Electron Spectrosc. Relat. Phenom.* 222, 40-50.
- 264 13. Sakho, I. (2018). *The Screening Constant by Unit Nuclear Charge Method:*
265 *Description and Application to the Photoionization of Atomic Systems.* London: ISTE
266 Science Publishing Ltd., & Hoboken, NJ: John Wiley & Sons, Inc.
- 267 14. Sharpee, B., et al. (2007). *The Astrophysical Journal*, 659(2), 1265–1275.
- 268 15. Sterling, N. C., et al. (2007). *The Astrophysical Journal Supplement Series*, 169(1),
269 37–65.
- 270 16. Sterling, N. C., & Dinerstein, H. L. (2008). *The Astrophysical Journal Supplement*
271 *Series*, 174(1), 158–186.

UNDER PEER REVIEW IN IJAR